THERMAL BEHAVIOR OF COPPER(II) 4-NITROIMIDAZOLATE

L. Ji-zhen[*], *F. Xue-zhong, H. Rong-zu, Z. Xiao-dong, Z. Feng-qi and G. Hong-Xu*

Xi'an Modern Chemistry Research Institute, Xi'an, Shaanxi 710065, China

The thermal behavior of copper(II) 4-nitroimidazolate (CuNI) under static and dynamic states are studied by means of high-pressure DSC (PDSC) and TG with the different heating rates and the combination technique of in situ thermolysis cell with rapid-scan Fourier transform infrared spectroscopy (thermolysis/RSFTIR).

The results show that the apparent activation energy and pre-exponential factor of the major exothermic decomposition reaction of CuNI obtained by Kissinger's method are 233.2 kJ mol^{-1} and $10^{17.95}$ s^{-1}, respectively. The critical temperature of the thermal explosion and the adiabatic time-to-explosion of CuNI are 601.97 K and 4.4~4.6 s, respectively. The decomposition of CuNI begins with the split of the C–NO$_2$ and C–H bonds, and the decomposition process of CuNI under dynamic states occurs less readily than those under static states because the dynamic nitrogen removes the strong oxidative decomposition product (NO$_2$). The above-mentioned information on thermal behavior is quite useful for analyzing and evaluating the stability and thermal charge rule of CuNI.

Keywords: copper(II) 4-nitroimidazolate, DSC, IR, kinetics, TG, thermolysis

Introduction

4-Nitroimidazole, an energetic material, which was studied as the intermediate of medicines [1–3], is found to be used as a main intermediate of dinitroimidazoles, trinitroimidazoles and metal 4-nitroimidazolates which can be used to improve the characteristics of cast explosives and solid propellants [4–8]. Copper(II) 4-nitroimidazolate (CuNI), a kind of new metal 4-nitroimidazolate, can be used as a main component, combustion catalyzer, of solid propellants. The study of thermal behavior is a very important starting point for the selection and exploitation of CuNI in applications, but there is no report on it until today.

The aim of this work is to study the thermolysis kinetics of CuNI under static and dynamic state and the real-time thermal decomposition [9] of CuNI by means of PDSC, TG [10–12] and the combination technique of in situ thermolysis cell with rapid-scan Fourier transform infrared spectroscopy (thermolysis/RSFTIR).

Experimental

Material

CuNI used in this work was prepared by Xi'an Modern Chemistry Research Institute, whose purity was more than 99.0%. Its structure is shown in Scheme 1.
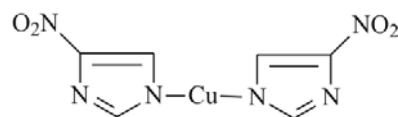
Scheme 1 Structure of CuNI

Experimental instruments and conditions

PDSC measurements were carried out on a Model DSC204 Netzsch instruments. The operation conditions were as follows: heating rates, 5, 10, 15, 20 and 40°C min^{-1}; sample mass, 0.5 to 1.0 mg; aluminium sample cell; atmosphere, static nitrogen with 1.0 MPa.

TG/DTG measurements were performed on a Model TA2950 TGA instruments. The conditions of TG/DTG were as follows: sample mass, 1.0 to 2.0 mg; heating rates, 5, 10, 15 and 20°C min^{-1}; atmosphere, flowing rate of N$_2$ gas, 60 mL min^{-1}.

Thermolysis/RSFTIR measurements were conducted using a Nicolet Model NEXUS 870 FT-IR Instrument and in situ thermolysis cell (Xiamen University, China) in the temperature range of 20~455°C and heating rate of 10°C min^{-1}. KBr pellet samples, well mixed by about 0.7 mg CuNI and 150 mg KBr, were used. Infrared spectra in the range of 4000~400 cm^{-1} were obtained by a model DTGS detector at a rate of 11 files min^{-1} and 8 scans file^{-1} with 4 cm^{-1} resolution.

The specific heat capacity (C_p, J mol^{-1} K^{-1}) of CuNI was determined with continuous C_p mode on a Micro-DSC III mircocalorimeter (Setaram Co., France).

---

* Author for correspondence: jizhenli@126.com

Results and discussion

The thermal decomposition behavior of CuNI under static N_2 gas conditions and flowing N_2 gas

The PDSC and TG curves for CuNI at different heating rates are shown in Figs 1 and 2. PDSC curves show that there are two exothermic peaks before 430°C. A major exothermic peak before 360°C is caused by the decomposition of CuNI. An exothermic process at the temperature of higher than 370°C is due to further decomposition of the decomposition products in coacervate phase. The TG curves also show two-stage mass loss processes.

Analysis of kinetic data

In order to obtain the kinetic parameters (the apparent activation energy E_a and pre-exponential constant A) of the major exothermic decomposition reaction of CuNI, a multiple heating method [13] (Kissinger's method) is employed. From the original data in Table 1, E_a is determined to be 233.21 kJ mol^{-1} and A as $10^{17.95}$ s^{-1}. The linear correlation coefficient (r_k) is 0.9868. The values of E_a and r_0 obtained by Ozawa's method [14] are 231.52 kJ mol^{-1} and 0.9879, respectively.

Under the condition of static N_2 gas, the value (T_{e0}) of the onset temperature (T_e) corresponding to β→0 by Eq. (1) taken from [15] using the data of T_e and β in Table 1 are 589.85 K,

$$T_{ei} = T_{e0} + b\beta_i + c\beta_i^2 + d\beta_i^3, \quad i=1, 2, \ldots, 5 \quad (1)$$

where, b, c and d are the coefficients.

The value of the critical temperature of thermal decomposition (T_b) obtained from Eq. (2) taken from [16] using the value of T_{e0} and E_o in Table 1 is 601.97 K,

$$T_b = \frac{E_o - \sqrt{E_o^2 - 4E_o R T_{e0}}}{2R} \quad (2)$$

where R is the gas constant (8.314 J mol^{-1} K^{-1}) and E_o the value of E obtained by Ozawa's method (231.5 kJ mol^{-1}).

From the original data in Tables 2 and 3, the value of E_a corresponding to the values of α for the thermal decomposition reaction under static and flowing N_2 gas conditions obtained by integral isoconversional non-linear (NL-INT) equation (3) [17]

$$\min = \left| \sum_{i}^{n} \sum_{j \neq i}^{n} \frac{\beta_j I(E_a, T_{a,i})}{\beta_i I(E_a, T_{a,j})} - n(n-1) \right| \quad (3)$$

are shown in Figs 3–4 and Tables 2–3. It is clear that the values of E_a do not seem to remain constant in the
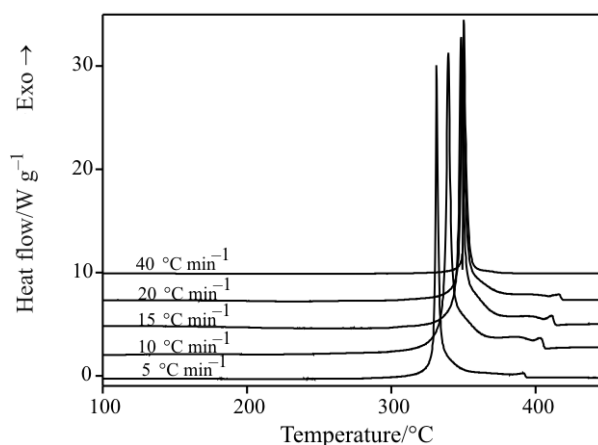

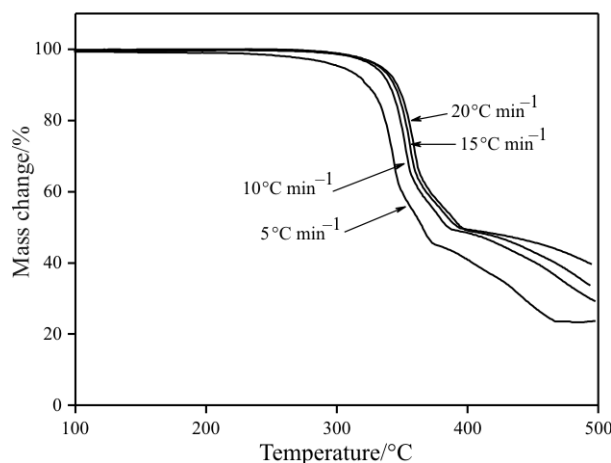**Fig. 1** PDSC curves of CuNI at different heating rates

Fig. 2 TG curves of CuNI at different heating rates

Table 1 Kinetic parameters of thermal decomposition of CuNI under static atmosphere calculated by Kissinger's method and Ozawa's method[*]

	β/K min^{-1}					$E_k{}^{a}$/ kJ mol^{-1}	$A_k{}^{a}$/ s^{-1}	r_k	$E_0{}^{b}$/ kJ mol^{-1}	r_0	T_{e0}/K	$T_b{}^{c}$/K
	5	10	15	20	40							
T_e/K	603.16	610.13	619.29	620.22	629.03				230.60	0.9891	589.85	601.97
T_p/K	604.54	612.75	621.56	622.33	630.56	233.21	$10^{17.95}$	0.9868	231.52	0.9879		

[*]T_e – onset temperature in the DSC curve; T_p – maximum peak temperature; β – heating rate; T_{eo} – the value (T_{eo}) of the onset temperature (T_e) corresponding to β→0 by Eq. (1); T_b – critical temperature of thermal explosion; E_a – apparent activation energy; A – pre-exponential constant; r – linear correlation coefficient; subscript k – data obtained by Kissinger's method; subscript o – data obtained by Ozawa's method. [a]Values of E_k and A_k calculated from the relationship of ln(β_i/T_{pi}^2) *vs.* 1/T_{pi}; [b]Values of E_o calculated from the relationship of lgβ_i *vs.* 1/T_{ei} or T_{pi}; [c]The value of T_b obtained from Eq. (2) using the data of E_o and T_{e0}.

decomposition process, but varied with the extent of conversion. This fact indicates that the thermal decomposition process of CuNI is a multiple reaction. Therefore, it is difficult to properly interpret the E_a dependence on α by means of kinetic mechanism.

Adiabatic time-to-explosion

The adiabatic time-to-explosion (t) of CuNI obtained from Eq. (4) taken from [18] is 4.6 s for $n=2$, 4.5 s for $n=1$ and 4.4 s for $n=0$.

Table 2 Apparent activation energies of thermal decomposition of CuNI under static N_2 gas condition obtained using integral isoconversional method

No.	α_i	T_i/K ($i=1, 2, \ldots, n$)					Eq. (3)	
		β/K min^{-1}					E_a/kJ mol^{-1}	min
		5	10	15	20	40		
1	0.125	602.13	609.11	617.75	619.51	629.12	224.76	0.1647
2	0.150	602.84	610.06	618.83	620.42	629.63	226.41	0.1835
3	0.175	603.16	610.74	619.57	620.96	629.86	227.19	0.2165
4	0.200	603.61	611.22	620.09	621.36	630.06	229.19	0.2243
5	0.225	603.86	611.60	620.47	621.63	630.24	229.94	0.2363
6	0.250	604.02	611.90	620.77	621.87	630.42	229.89	0.2443
7	0.275	604.18	612.14	621.01	622.04	630.57	230.12	0.2512
8	0.300	604.31	612.38	621.22	622.26	630.75	229.89	0.2517
9	0.325	604.43	612.60	621.45	622.45	630.92	229.53	0.2578
10	0.350	604.55	612.83	621.65	622.66	631.06	229.45	0.2610
11	0.375	604.66	613.06	621.84	622.84	631.27	228.95	0.2590
12	0.400	604.77	613.31	622.09	623.05	631.47	228.32	0.2694
13	0.425	604.89	613.55	622.33	623.27	631.70	227.56	0.2688
14	0.450	605.01	613.84	622.59	623.52	631.87	227.20	0.2777
15	0.475	605.22	614.22	622.92	623.79	632.09	227.53	0.2887
16	0.500	605.38	614.67	623.30	624.08	632.33	226.89	0.3068
17	0.525	605.58	615.33	623.78	624.43	632.60	226.71	0.3366
18	0.550	605.81	616.14	624.42	624.84	632.88	226.27	0.3984
19	0.575	606.08	617.19	625.25	625.34	633.20	225.29	0.5066
20	0.600	606.45	618.45	626.30	625.97	633.55	223.79	0.6787
21	0.625	606.88	619.90	627.56	626.80	633.97	220.78	0.9225
22	0.650	607.48	621.49	629.00	627.90	634.44	217.24	1.2270
23	0.675	608.27	623.26	630.60	629.24	635.00	213.28	1.5894
24	0.700	609.31	625.17	632.34	630.87	635.70	209.38	1.9804
25	0.725	650.60	627.33	634.28	632.77	636.59	205.04	2.4209
26	0.750	612.12	629.82	636.51	634.91	637.85	199.44	2.8883
27	0.775	613.89	632.76	639.13	637.35	639.57	192.16	3.3837
28	0.800	616.00	636.40	642.39	640.25	641.84	182.23	3.9698
29	0.825	618.61	640.83	646.55	643.86	644.63	169.40	4.7110
30	0.850	622.00	645.79	651.57	648.63	648.01	156.82	5.4525
31	0.875	626.57	650.90	657.01	654.65	652.21	150.51	5.9119
32	0.900	632.55	655.95	662.55	661.36	658.08	156.75	5.6401
33	0.925	639.47	660.90	668.02	668.21	667.65	178.73	3.7473
34	0.950	647.41	666.14	673.69	675.35	680.52	195.09	1.3009
35	0.975	657.19	672.64	680.63	683.92	693.99	199.72	0.2688
36	1.000	668.00	680.59	688.76	694.11	710.91	211.11	4.7121

*α_i – the degree of CuNI decomposition; min, the minimum on the right side of Eq. (3)

$$t = \int_{T_0}^{T} \frac{C_p \exp(E/RT)}{QAf(\alpha)} dT \qquad (4)$$

where C_p, specific heat capacity, $C_p = -0.02176296 + 0.0031686811T$, K; $f(\alpha)$, differential mechanism function $f(\alpha) = (1-\alpha)^n$; n, the rate order; E, apparent activation energy, $E_a = 233210$ J mol^{-1}; A, pre-exponential constant, $A = 10^{17.95}$ s^{-1}; Q, heat of decomposition, $Q = 1644$ J g^{-1}; R, the gas constant, $R = 8.314$ J mol^{-1} K^{-1}; α, the conversion degree, $\alpha = \int_{T_0}^{T} (C_p/Q) dT$; T, the integral upper limit, $T = T_b = 601.92$ K; T_0, the lower limit, $T_0 = T_{e0} = 289.85$ K.

Table 3 Apparent activation energies of thermal decomposition of CuNI under flowing N$_2$ gas conditions obtained using integral isoconversional method

No.	α_i	T_i/K (i=1, 2, …, n) β/K min^{-1}				Eq. (3)	
		5	10	15	20	E_a/kJ mol^{-1}	min
1	0.125	573.31	599.55	602.52	603.65	101.94	0.6042
2	0.150	580.42	602.94	606.01	607.49	120.86	0.5148
3	0.175	585.18	605.56	608.78	610.58	134.27	0.4385
4	0.200	589.15	607.74	610.97	613.04	147.71	0.3787
5	0.225	592.37	609.56	612.87	615.06	159.63	0.3302
6	0.250	594.17	611.05	614.46	616.65	162.70	0.3149
7	0.275	596.51	612.43	615.83	618.09	172.48	0.2855
8	0.300	598.99	613.59	617.03	619.38	186.68	0.2398
9	0.325	600.99	614.68	618.09	620.48	198.35	0.2125
10	0.350	602.66	615.62	619.06	621.50	208.05	0.1851
11	0.375	604.10	616.49	619.94	622.44	216.24	0.1631
12	0.400	605.32	617.28	620.75	623.28	222.80	0.1468
13	0.425	606.42	618.05	621.42	624.09	228.73	0.1344
14	0.450	607.37	618.74	622.11	625.00	231.86	0.1149
15	0.475	608.26	619.38	622.77	625.51	237.31	0.1138
16	0.500	609.07	620.00	623.40	626.14	240.89	0.1075
17	0.525	609.81	620.57	624.01	626.75	243.74	0.1002
18	0.550	610.54	621.14	624.56	627.31	247.21	0.0959
19	0.575	611.18	621.66	625.08	627.86	249.53	0.0909
20	0.600	611.79	622.16	625.59	628.38	251.71	0.0867
21	0.625	612.39	622.65	626.06	628.87	254.26	0.0836
22	0.650	612.94	623.13	626.53	629.35	256.02	0.0816
23	0.675	613.50	623.58	626.98	629.80	258.48	0.0784
24	0.700	613.99	624.02	627.40	630.26	259.73	0.0762
25	0.725	614.49	624.47	627.82	630.69	261.45	0.0758
26	0.750	614.97	624.88	628.22	631.12	263.02	0.0731
27	0.775	615.44	625.29	628.61	631.52	264.77	0.0719
28	0.800	615.90	625.70	629.02	631.93	266.12	0.0705
29	0.825	616.35	626.10	629.40	632.34	267.48	0.0689
30	0.850	616.81	626.49	629.77	632.74	269.24	0.0668
31	0.875	617.23	626.87	630.15	633.14	270.17	0.0650
32	0.900	617.68	627.28	630.53	633.54	271.63	0.0646
33	0.925	618.12	627.67	630.92	633.97	272.56	0.0618
34	0.950	618.61	628.08	631.33	634.43	274.01	0.0581
35	0.975	619.13	628.58	631.82	634.94	274.81	0.0575
36	1.000	619.70	629.20	632.37	635.53	275.09	0.0608

Thermolysis in the slowly heated IR cell

Thermolysis/RSFTIR was used to analyze the condensed phase products of the thermal decomposition of CuNI under the linear temperature rise condition in real time.

The RSFTIR spectrum of CuNI at room temperature is shown in Fig. 5. The antisymmetric and symmetric stretching vibration absorptions of $C-NO_2$ bonds
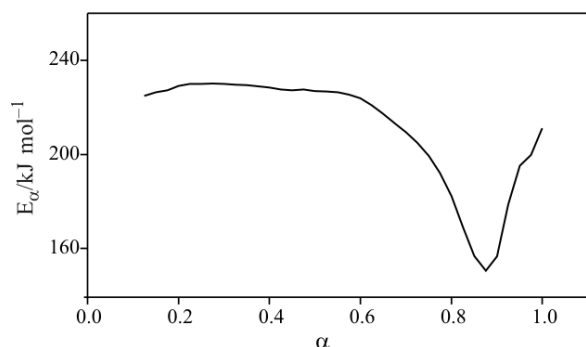
$(\upsilon_{as(C-NO_2)}$ and $\upsilon_{s(C-NO_2)})$ at 1525 and 1382 cm^{-1}, the $\upsilon_{as(C-H)}$ and $\upsilon_{s(C-H)}$ peaks at 3169 and 3111 cm^{-1} for the C–H bonds, the $\upsilon_{C=C}$ and $\upsilon_{C=N}$ peaks at 1495 and 1458 cm^{-1} for the C=C and C=N bonds, the δ_{C-H} in the plane at 1275–975 cm^{-1} for the C–H bonds, and the δ_{C-H} perpendicular to the plane at lower than 900 cm^{-1} for the C–H bonds can be observed from Fig. 5.

The IR spectra of CuNI at different temperatures are shown in Fig. 6. It can be clearly seen that the intensity of the $\upsilon_{as(C-H)}$, $\upsilon_{s(C-H)}$, $\upsilon_{as(C-NO_2)}$ and $\upsilon_{s(C-NO_2)}$, $\upsilon_{C=C}$ and $\upsilon_{C=N}$ peaks at 3169, 3111, 1525, 1382, 1495 and 1458 cm^{-1} weaken rapidly at the temperature of about 250°C, and the swift absorption peaks at 3169, 2361, 2336, 2165 and 1612 cm^{-1} emerge. The intensity of all the other characteristic absorption peaks weaken and disappear at 455.4°C, except for the characteristic absorption peaks of CO_2 at 2336, 2361 and 670 cm^{-1} and CO at 2165 cm^{-1}.

The characteristic absorption peaks of CuNI and its condensed phase products are chosen to make the intensity vs. temperature curves. In Fig. 7, the disappearance of the $\upsilon_{as(C-NO_2)}$ and $\upsilon_{s(C-NO_2)}$ peaks (1382 and 1525 cm^{-1}) and the emergence of υ_{NO_2} peaks (1612 cm^{-1}) are easily recognized in the temperature

Fig. 3 The relation between E_a and α for the thermal decomposition reaction of CuNI under static N_2 gas conditions at 1.0 MPa
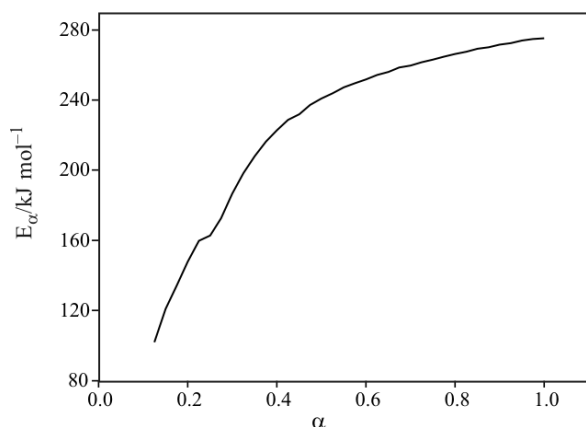
Fig. 4 The relation between E_a and α for the thermal decomposition reaction of CuNI under flowing N_2 gas conditions at a flow rate of 60 mL min^{-1}

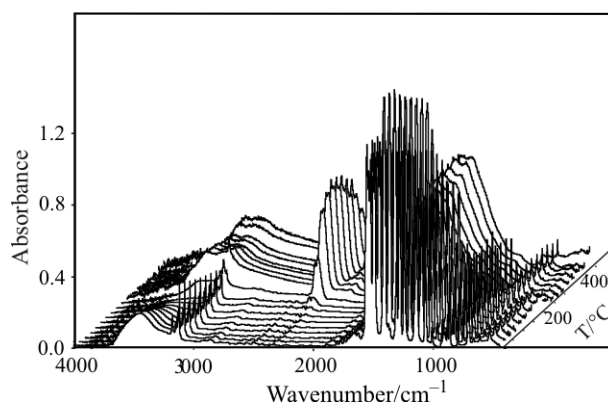**Fig. 5** RSFTIR spectrum of CuNI at room temperature

Fig. 6 The typical IR spectra of the condensed products at different temperatures during the thermal decomposition process of CuNI
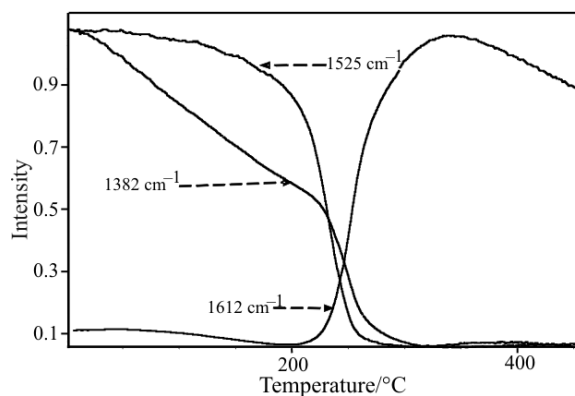

Fig. 7 Intensity vs. temperature curves of the characteristic absorption peaks at 1382, 1525 and 1612 cm^{-1}

range of 220–260°C, and in Fig. 8, the disappearance of the $\upsilon_{C=C}$ and $\upsilon_{C=N}$ peaks (1495 and 1458 cm^{-1}) are easily seen in the temperature range of 230–300°C. Therefore, the C–NO$_2$ bonds of CuNI are broken in the temperature range of 220–260°C, whose strong oxidative product NO$_2$ destroy the unstable annulus of CuNI (the C=C and C=N bonds are broken in the temperature range of 230–300°C).

It can be seen from Fig. 9 that the intensity of the $\upsilon_{as(C–H)}$, $\upsilon_{s(S–H)}$ and $\delta_{C–H}$ peaks decrease rapidly in the temperature range of 220–260°C, and in the tempera-
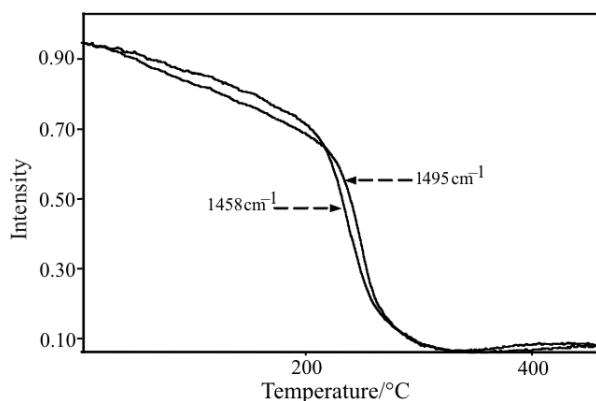
Fig. 8 Intensity *vs.* temperature curves of the characteristic absorption peaks at 1458 and 1495 cm^{-1}
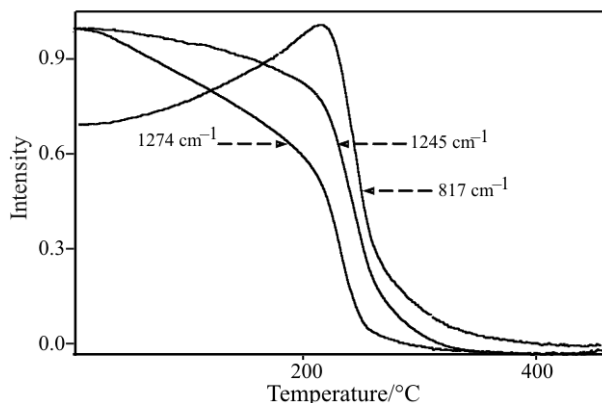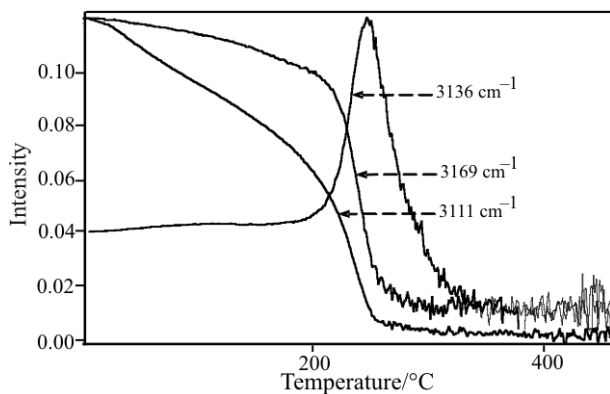

Fig. 9 Intensity *vs.* temperature curves of the characteristic absorption peaks at 817, 1245, 1274, 3111, 3136 and 3169 cm^{-1}
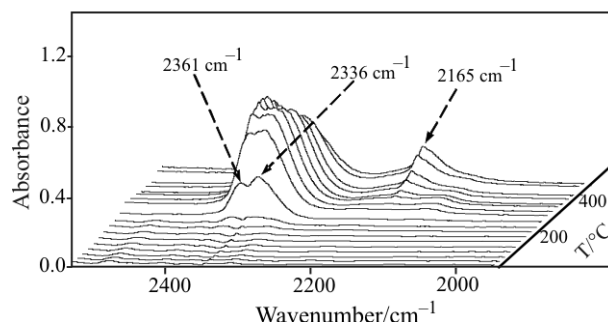

Fig. 10 Changes in the characteristic absorption peaks at 2165, 2336 and 2361 cm^{-1} during the thermal decomposition process of CuNI
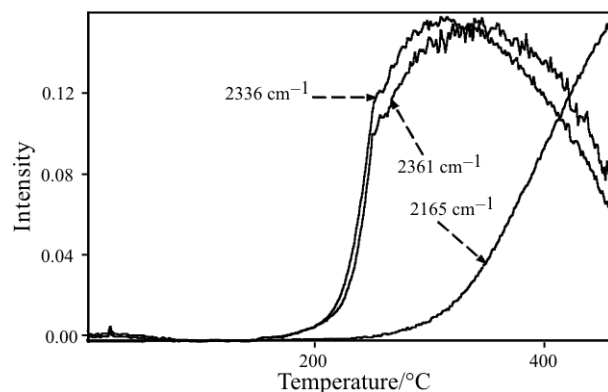

Fig. 11 Intensity *vs.* temperature curves of the characteristic absorption peaks at 2336, 2361 and 2165 cm^{-1}

ture range of 220–250°C, the $\upsilon_{s(C–H)}$ peak at 3111 cm^{-1} combines with the $\upsilon_{as(C–H)}$ peak at 3169 cm^{-1} forming an absorption peak at 3136 cm^{-1}.

In Figs 10 and 11, it is easily observed that the oxides of carbon, gas products of CuNI decomposition, contain CO$_2$ and CO, which characteristic absorption peaks ($\upsilon_{as(CO_2)}$, $\upsilon_{s(CO_2)}$ and υ_{CO}) at 2336, 2361 and 2165 cm^{-1} emerge from about 220 and 310°C, respectively.

Thus, the C–NO$_2$ and C–H bonds of CuNI are broken with the increase in temperature simultaneously, whose strong oxidative product (NO$_2$) destroy the unstable annulus of CuNI instantly, and finally, the conjugated C=C and C=N bonds of the five-membered ring are broken. It confirmed the result of the two exothermic peaks on PDSC and the two-stage mass loss processes of TG curves of CuNI. The gas products of CuNI decomposition consist of NO$_2$, CO$_2$ and CO.

Because of the different test conditions, the temperature data of thermolysis/RSTFIR are different from those of DSC and TG-DTG. Thus, thermolysis/RSTFIR measurement is used to make qualitative analysis, while PDSC measurement is employed to make quantitative analysis.

Conclusions

- The extrapolated onset temperature corresponding to β→0 of the major exothermic process (T_{e0}) is 589.85 K.
- The critical temperature of thermal explosion of CuNI (T_b) is 601.97 K.
- The adiabatic time-to-explosion from T_{e0} to T_b is about 4.4–4.6 s.
- The apparent activation energy (E_a) and pre-exponential constant (A) of the major exothermic decomposition reaction of CuNI obtained by a multiple heating method are 233.21 kJ mol^{-1} and $10^{17.95}$ s^{-1}, respectively.
- The values of E_a in decomposition process variate with the extent of conversion (α) indicating that it is difficult to properly interpret the E_a dependence on α by means of kinetic mechanism.
- The decomposition of CuNI, which contain two steps with the temperature rise, begins with the split of C–NO$_2$ and C–H bonds. The gas products detected of CuNI decomposition consist of NO$_2$, CO$_2$ and CO.
- The decomposition process of CuNI under dynamic states occurs less readily than those under static states because of the dynamic nitrogen taking off the strong oxidative decomposition product (NO$_2$).

References

1 T. Chu, S. Hu, B. Wei, Y. Wang, X. Liu and X. Wang, Bioorg. Med. Chem. Lett., 14 (2004) 747.
2 S. R. Tannenbaum, Biochem., 41 (2002) 7508.
3 L. Jia, V. Shafirovich, R. Shapiro, N. E. Geacintov and S. Broyde, Biochem., 45 (2006) 6644.
4 D. Reddy and J. Keerti, USP 5387297, 1993.
5 A. J. Bracuti, J. Chem. Cryst., 28 (1998) 367.
6 J. R. Cho, K. J. Kim, S. G. Cho and J. K. Kim, J. Hetero. Chem., 39 (2002) 141.
7 J. R. Cho, S. G. Cho, K. J. Kim and J. K. Kim, Insensitive Munitions & Energetic Materials Technology Symposium, NDIA, San Diego 2000, p. 393.
8 S. Jerzy and S. Ewa, Pol. J. Chem., 61 (1987) 613.
9 J. Z. Li, G. F. Zhang, X. Z. Fan, R. Z. Hu and Q. Pan, J. Anal. Appl. Pyrolysis, 76 (2006) 1.
10 S. C. Mojumdar, G. Madgurambal and M. T. Saleh, J. Therm. Anal. Cal., 81 (2005) 205.
11 G. Z. Papageorgiou, D. S. Achilias, D. N. Bikiaris and G. P. Karayannidis, J. Therm. Anal. Cal., 84 (2006) 85.
12 Y. J. Wan, L. Q. Li and D. H. Chen, J. Therm. Anal. Cal., 90 (2007) 415.
13 H. E. Kissinger, Anal. Chem., 29 (1957) 1702.
14 T. Ozawa, Bull, Chem. Sec. Jpn., 38 (1965) 1881.
15 R. Z. Hu and Q. Z. Shi, Thermal Analysis Kinetics, Science Press, Beijing 2001, p. 127.
16 T. L. Zhang, R. Z. Hu, Y. Xie and F. P. Li, Thermochim. Acta, 244 (1994) 171.
17 R. Z. Hu, F. Q. Zhao, H. X. Gao, H. Zhang and Q. C. Song, Chin. J. Energ. Mater., 19 (2007) 97.
18 R. Z. Hu, S. L. Gao, F. Q. Zhao, Q. Z. Shi, T. L. Zhang and J. J. Zhang, Thermal Analysis Kinetics, Science Press, Beijing 2007, p. 342.